Experimentally realizable controlled NOT gate in a flux qubit/resonator system

Shiro Saito,[1,*] Todd Tilma,[2,†] Simon J. Devitt,[2] Kae Nemoto,[2] and Kouich Semba[1]
[1]*NTT Basic Research Laboratories, NTT Corporation, 3-1 Morinosato-Wakamiya, Atsugi-shi, Kanagawa-ken 243-0198, Japan*
[2]*National Institute of Informatics, 2-1-2 Hitotsubashi, Chiyoda-ku, Tokyo-to 101-8430, Japan*
(Received 6 April 2009; published 14 December 2009)

We present an experimentally realizable microwave pulse sequence that effects a controlled-NOT (C-NOT) gate operation on a Josephson-junction-based flux qubit/resonator system with high-process fidelity. We obtained a C-NOT gate process fidelity of 0.988 (0.980) for a two-(three-)qubit/resonator system under ideal conditions and a fidelity of 0.903 for a two-qubit/resonator system under the best, currently achieved, experimental conditions. Our simulations show that this gate is a feasible first step toward multiqubit quantum-information processing with flux qubit/resonator systems.

DOI: 10.1103/PhysRevB.80.224509 PACS number(s): 74.50.+r, 03.67.Lx, 85.25.Cp

I. INTRODUCTION

The basic requirements for a successful quantum computer have been expressed by DiVincenzo[1,2] nearly a decade ago. These five criteria have been widely accepted as being the best road map for achieving realizable quantum computing by most research programs throughout the world: (1) a scalable physical system of well-characterized qubits. (2) The ability to initialize the state of the qubits to a simple fiducial state. (3) Long (relative) coherence times, much longer than the gate-operation time. (4) A universal set of quantum gates. (5) A qubit-specific measurement capability.

At this time, there are various schemes being proposed to satisfy the above criteria and realize a quantum computer.[3] At the few-qubit level, these schemes include those based on trapped ions,[4] liner optics,[5,6] and nuclear spins in liquid-state molecules.[7,8] For the long-term prospects of scalability though, those schemes that utilize Josephson-junction-based qubits[9] have significant advantages.

Since the initial breakthrough in the coherent manipulation of a single Josephson-junction-based charge qubit nearly a decade ago,[9] the experimental focus has widely extended to the creation, control, and subsequent manipulation of, multiqubit entanglement in similar Josephson-junction-based systems. For example, coherent oscillations between two qubits have been observed by using a fixed interqubit coupling.[10–12] However, the fixed nature of the qubit-qubit coupling used in these experiments makes it difficult to scale up such circuits in the future. To overcome this problem, a fast switchable coupling between two qubits has been proposed[13–15] and also demonstrated.[16,17]

Beyond direct qubit-qubit couplings, another solution is to make use of a quantum bus (qubus) as a coupler between qubits.[18–20] Using the qubus concept we can perform any two-qubit operation, between any two qubits that are coupled to the bus, without using multiple swap gates, which are necessary in other systems using direct qubit-qubit coupling. In particular, harmonic oscillators formed by superconducting circuits seem to be a good candidate for a qubus-type coupler. Early experiments with such couplers have shown coherent oscillations between a qubit and the oscillator, which was made of lumped elements, namely, capacitors and inductors.[21,22] More recently, a distributed circuit, based on a coplanar waveguide resonator, attracted considerable attention as an oscillator because of its high-quality factor (Q factor) and impedance matching to other circuits.[23,24] Furthermore, coherent quantum state transfer between two Josephson-junction-based qubits via such a waveguide resonator has been demonstrated in both the phase[25] and charge regime.[26] More recently, two-qubit algorithms have been demonstrated in a two-transmon qubit/resonator system.[27]

Because of the experimental viability of the qubus-coupler concept, as well as its obvious advantages in scalability, we are using this paper to propose an experimentally realizable microwave pulse sequence that will enact a controlled NOT (C-NOT) gate between two superconducting flux qubits, which are coupled via a harmonic-oscillator bus. This pulse sequence/flux qubit/resonator design is complementary to other recently proposed systems[18,28] but stands apart due to its efficiency of operation and its process fidelity.

II. EXPERIMENTAL SYSTEM

One of the most promising solid-state quantum-computing elements is a superconducting flux qubit that typically consists of three Josephson junctions in a loop: two of equal size, one smaller by a factor $\alpha \simeq 0.8$.[29] The sizes of the junctions are chosen so that the geometric self-inductance of the loop is not physically relevant. The two lowest-energy states of the qubit at the flux degeneracy point, usually denoted as $|0\rangle$ and $|1\rangle$, are superpositions of macroscopically distinct clockwise and counter-clockwise persistent current states. Repeated experiments over the past few years have shown that this type of flux qubit is a well-defined quantum system that can perform single-qubit rotations[30–34] as well as achieve long coherence times of a few microseconds.[32] In order to exploit these quantum properties and avoid decoherence due to flux fluctuations, it is desired to operate the flux qubits at the degeneracy point.[32–34]

We are currently working with the following architecture (see Fig. 1) built around the previously discussed three Josephson-junction qubit design that incorporates the fundamentals of the qubus concept. Each qubit couples to the resonator through a mutual inductance M. Here the resonator is schematically represented by lumped elements but it can be a

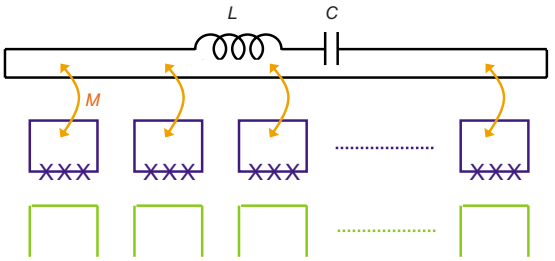

FIG. 1. (Color online) Multiple flux qubits (blue rectangles with three crosses), each addressed by its own microwave line (green line), coupled to a resonator via a mutual inductance M. The resonator is schematically represented by the inductor L and the capacitor C.

distributed circuit, for example, a coplanar strip waveguide. External magnetic flux through each qubit is a half-flux quanta in order to set the qubits at the degeneracy point.

III. C-NOT PULSE SEQUENCE

In order to execute a C-NOT gate in our architecture we have to entangle the flux qubits with the resonator. To do this, we need to apply a sequence of dc-shift pulses or apply a sequence of microwave pulses through microwave lines to our qubits. In the case of dc-shift pulses, we can adiabatically change the qubit frequency to fit the resonator frequency but also nonadiabatically in order to create a coupling between the qubit and the resonator. As a result, we can "turn on" the coupling between the qubit and the resonator nonadiabatically, making them into an entangled state.[22,25] However, these pulses cause dc-based excursions away from the flux degeneracy point and can reduce the dephasing times of the qubits drastically. The large bandwidth of the pulses can also reduce the overall process fidelity. Fortunately, a special flux qubit design combined with elaborate dc pulses may solve these problems.[28]

When we use a sequence of microwave pulses, we can create entanglement between the qubits and the resonator by using a known two-photon blue side band (BSB) transition at the qubit's degeneracy point.[18,35] These microwave pulses have a more narrower bandwidth than the dc-shift pulses thus allowing us to obtain a much higher process fidelity as well as minimizing pulse-induced dephasing. For example, high-process fidelity C-NOT gate operations have been achieved in ion-trap experiments using such BSB transitions.[36,37] In these experiments, an elaborate controlled-Z gate using four BSB pulses was used.[4]

Our C-NOT gate in this paper is also based on BSB transitions. However, it is difficult to achieve similar high-process fidelity because of the strong fixed coupling between the qubit and the resonator. This coupling leads to larger energy shifts at higher energy levels, represented by the solid and dashed lines in Fig. 2(a). These shifts are problematic if we want to implement a Cirac-Zoller-type C-NOT gate. Indeed, such a BSB-based C-NOT gate uses up to $n=2$ resonator levels, where n is the photon number in the resonator.[4] By contrast, our C-NOT gate design exploits our strong fixed coupling to realize a high-fidelity controlled-Z gate through

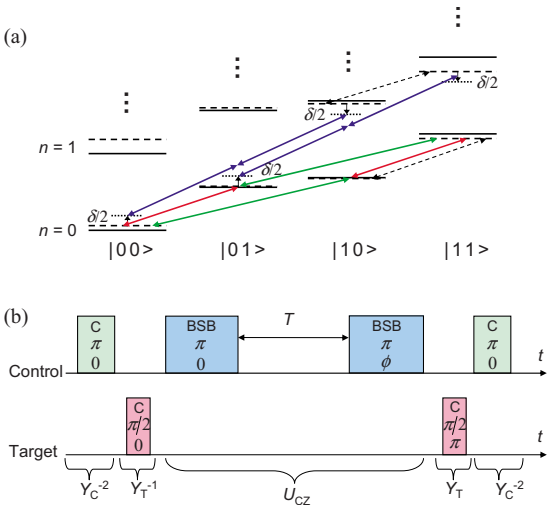

FIG. 2. (Color online) (a) Energy levels of the two-qubit/resonator system and transitions used in our pulse sequence. Solid (dashed) lines represent the energy levels without (with) the coupling between the qubits and the resonator. Additional shifts δ occur during the irradiation of the BSB pulse. Energy difference between the dashed arrows is utilized to perform the controlled-Z gate between the resonator and the target qubit. (b) Basic operational sequence of target, control, and BSB pulses on our two qubits, using values defined in Sec. IV, that enact a C-NOT gate in our system. Each pulse is represented by the microwave frequency (carrier frequency or BSB frequency), the rotation angle, and the phase of the microwave pulse. Note that the parameters T, the free evolution time, and ϕ, the microwave pulse phase, are variable and are defined by the experimental system to those values that optimize the operation of the gate. Unitary matrix representations of each pulse are shown by Y_C, Y_T, and U_{CZ}, which are also used in Eq. (1).

BSB transitions between the two lowest levels ($n=0,1$) of the resonator. In this way, a pulse sequence for a C-NOT gate can be constructed based around these transitions [see Fig. 2(b)].

To realize our BSB-based controlled-Z gate, we take for granted that the resonator is in the $n=0$ state at the beginning. This is easy to realize in superconducting circuits because the energy scale due to the typical temperature of a sample (30 mK) is much lower than the energy difference between resonator levels. As the two-concatenated blue arrows in Fig. 2(a) show, the first BSB π pulse changes the state $|00\rangle$ (in the $n=0$ level) to $|10\rangle$ (in the $n=1$ level) and changes the state $|01\rangle$ (in the $n=0$ level) to $|11\rangle$ (in the $n=1$ level), where $|CT\rangle=|C\rangle|T\rangle$ and $|C\rangle$ ($|T\rangle$) represents the state of the control (target) qubit. As a result of this pulse the state of the control qubit is mapped to the resonator. This temporarily changes our gate basis from $|00\rangle$, $|01\rangle$, $|10\rangle$, $|11\rangle$ (in the $n=0$ level) to $|10\rangle$, and $|11\rangle$ (in both the $n=0$ and $n=1$ levels).

At this point it is important to note that the speed of the phase evolution on the control qubit is different between the $n=0$ and $n=1$ levels because of the energy difference indicated by the two dashed arrows in Fig. 2(a). Therefore, after a time interval T, only the $|11\rangle$ state (in the $n=1$ level) will acquire a π phase, relative to the other three basis states. This free evolution functions as a controlled-Z gate between

the resonator and the target qubit. Similar gate operations have been employed in nuclear magnetic resonance quantum computation.[38]

In order to achieve a controlled-Z gate between the control and target qubits, a second BSB π pulse is needed to transfer the phase information on the resonator back to the control qubit and disentangle the resonator from the qubits. The phase difference between this pulse and the first BSB pulse must be carefully adjusted in order to cancel the effect of the off-resonant ac-Stark shift δ shown in Fig. 2(a).[18] The two BSB pulses, with appropriate phases, place an additional dynamical phase π on the $|00\rangle$ and $|01\rangle$ states (in the $n=0$ level). In the end, these two BSB π pulses, combined with the free evolution time T, work as a controlled-Z gate between the two qubits (U_{CZ}).

Finally, the U_{CZ} gate together with four single-qubit gates forms the C-NOT gate ($U_{\text{C-NOT}}$)

$$U_{\text{C-NOT}} = Y_C^{-2} Y_T U_{CZ} Y_T^{-1} Y_C^{-2} = -\begin{pmatrix} 0 & 1 & 0 & 0 \\ 1 & 0 & 0 & 0 \\ 0 & 0 & 1 & 0 \\ 0 & 0 & 0 & 1 \end{pmatrix} \tag{1}$$

in the two-qubit basis $\{|11\rangle, |10\rangle, |01\rangle, |00\rangle\}$. Here, Y_C and Y_T represent a $\pi/2$ gate on the control, and the target, qubit, respectively. We should note that during the whole pulse sequence, we only use six states, namely, the four states in the $n=0$ resonator level and $|10\rangle$ and $|11\rangle$ in the $n=1$ resonator level.

IV. NUMERICAL SIMULATIONS

In this section, our focus will be on simulating those pulses that implement our high-fidelity C-NOT gate upon any two qubits in our architecture (Fig. 1). To begin, when all the qubits in our system are at their respective degeneracy points, the overall system is represented by the following Hamiltonian:

$$H = hf_{\text{res}} a^\dagger a + \sum_k \left[\frac{1}{2} hf_k \sigma_{z,k} + hg_k \sigma_{x,k} (a^\dagger + a) + hA_{\text{MW},k} \sin(\omega_k t + \phi_k) \sigma_{x,k} \right]. \tag{2}$$

Here, h is Planck's constant, f_{res} is the frequency of our resonator, $\frac{1}{2} hf_k \sigma_{z,k}$ represents the "kth" qubit, $hg_k \sigma_{x,k}(a^\dagger + a)$ is the coupling term between the kth qubit and the resonator, and $hA_{\text{MW},k} \sin(\omega_k t + \phi_k)\sigma_{x,k}$ describes the microwave pulse for each qubit. Since we are only looking at C-NOT gates, we will define one qubit as the target and one as the control qubit.

Using the above time-dependent Hamiltonian we will evaluate how accurately our pulse sequence describes a C-NOT gate on any two qubits. Our simulated gate, including error sources, can be described by a completely positive map ε from an initial density matrix ρ_{in} to an output state ρ_{out}. Hence, ρ_{out} can be written in the operator sum representation as[39]

$$\rho_{\text{out}} = \varepsilon(\rho_{\text{in}}) = \sum_{m,n} \tilde{E}_m \rho_{\text{in}} \tilde{E}_n^\dagger \chi_{mn}, \tag{3}$$

where $\tilde{E}_m$ are operators forming a basis in the space of 4×4 matrices.

Equation (4) shows that ε can be completely described by a complex number matrix χ once the set of operators $\tilde{E}_m$ has been fixed. The operators $\tilde{E}_m$ can be represented by

$$\tilde{E}_{4i+j} = A_i \otimes A_j, \tag{4}$$

where A_i is a set of operators forming a basis in the space of single-qubit operators. In this work, we have chosen $A_0 = I$, $A_1 = \sigma_x$, $A_2 = \sigma_y$, and $A_3 = \sigma_z$. To determine χ, which is a 16×16 matrix, we need to simulate our gate for 16 linearly independent input states $|\psi_{\text{in}}\rangle$. For these states we have chosen

$$|\psi_{\text{in}}\rangle = |\psi_i\rangle \otimes |\psi_j\rangle,$$
$$|\psi_i\rangle \in \{|0\rangle, |1\rangle, (|0\rangle + |1\rangle)/\sqrt{2}, (|0\rangle + i|1\rangle)/\sqrt{2}\} \tag{5}$$

as the initial states. From this we can evaluate the gate fidelity using the process fidelity

$$F_p = \text{Tr}(\chi_{\text{ideal}} \chi_{\text{sim}}), \tag{6}$$

where χ_{ideal} and χ_{sim} represent the ideal matrix, and the one obtained from the simulation, respectively.

Our two qubits (the target and control) and resonator operating frequencies, as well as couplings, were defined in the following way:[40]

$$\begin{aligned} &f_1 = f_{\text{Control}} = 6 \text{ GHz} \quad g_1 = 0.1 \text{ GHz}, \\ &f_2 = f_{\text{Target}} = 5 \text{ GHz} \quad g_2 = 0.1 \text{ GHz}, \\ &f_{\text{res}} = 10 \text{ GHz}. \end{aligned} \tag{7}$$

For our numerical simulations we used the following values for our target and control pulses:

Target Pulse	Control Pulse
$A_{\text{MW},2} = 0.1$ GHz	$A_{\text{MW},1} = 0.1$ GHz
$\omega_2/2\pi = 4.99875$ GHz	$\omega_1/2\pi = 5.9981$ GHz
$\phi = 0$ or π	$\phi = 0$

(8)

as well as our BSB pulses

Control BSB
$A_{\text{MW},1} = 2$ GHz
$\omega_1/2\pi = 7.5601$ GHz
$\phi = 0$ or 0.34π.

(9)

Here the rise/fall time of each pulse was set at 0.8 ns and the duration of the carrier $\pi(\pi/2)$ pulse was set at 5 (2.5) ns. As mentioned in Sec. III, we optimized the duration of the BSB pulse, the free evolution time T, and the phase of the second BSB pulse ϕ in order to achieve the best process fidelity, obtaining 16.295 ns, 162.865 ns, and 0.34π, respectively. The total length of the pulse sequence is about 200 ns, which is much shorter than the coherence time of a flux qubit.[32] Lastly, we assumed that the first five resonator levels were

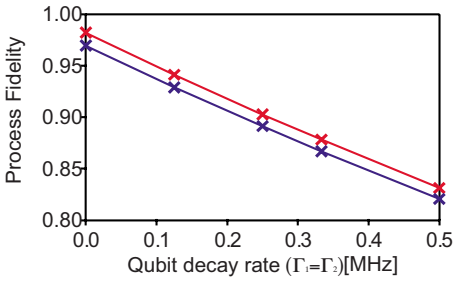

FIG. 3. (Color online) Process fidelity as a function of qubit decay rate. The upper (lower) curve represents the fidelity when the quality factor of the resonator is $10^6(3\times10^5)$.

accessible, thus $n=0$ to $n=4$, where n is the photon number in the resonator.

V. OBSERVATION AND ANALYSIS

Multiple simulations, using the previously defined parameters with various pulse shapes and operation times, have yielded an experimentally realizable pulse sequence, represented in Fig. 2(b), that will enact a C-NOT gate upon our two-qubit/resonator system with high process fidelity, $F_p=0.988$, and within the coherence time of known flux qubit systems.[32] The computed gate (to four significant figures) is

$$U'_{\text{C-NOT}} = -\begin{pmatrix} 0.0001 & 0.9863 & 0.0013 & 0.0022 \\ 0.9863 & 0.0001 & 0.0020 & 0.0013 \\ 0.0021 & 0.0014 & 0.9886 & 0.0034 \\ 0.0013 & 0.0023 & 0.0035 & 0.9880 \end{pmatrix}. \tag{10}$$

We also evaluated the effects of decoherence on our C-NOT gate by introducing a linear loss to the resonator (quality factor Q), as well as relaxation rates Γ_1 and dephasing rates Γ_2 to the qubits, via a master equation of the Lindblad form (see Figs. 3 and 4). Here we assumed that Γ_1 and Γ_2 for both qubits were equal. We obtained a process fidelity of 0.903 under the best conditions that have been achieved experimentally: $Q=10^6$ and $\Gamma_1=\Gamma_2=0.25$ MHz. Even with this realistic decoherence model, our process fidelity is still more than 90%, showing our gate remains robust against this type of loss.

Now, in the case of flux qubits, it is difficult to fabricate a qubit which has an exactly designed gap frequency at the degeneracy point unless the qubit uses a controllable third junction.[41] Hence, we also simulated the case in which the two-qubit frequencies drew closer. When $f_{\text{res}}=10$ GHz, $f_{\text{Control}}=6$ GHz, and $f_{\text{Target}}=5.5$ GHz, we obtained a process fidelity of 0.986 without decoherence. Decreasing the difference between the two-qubit frequencies did not significantly affect the fidelity.

Our C-NOT gate also works with any two qubits in a system with many qubits since we can effectively decouple any unused qubits from the resonator. Although we have a fixed coupling between the qubits and the resonator, when the resonator is in the $n=0$ level, it does not affect the qubit states and hence the gate fidelity. Here we ignore the qubit-qubit coupling via the resonator, which is at most 10 kHz. This is much smaller than the inverse of our gate time. During the free evolution time between the first and second BSB pulse, the fixed coupling could induce unwanted phase on the unused qubits. However, we can eliminate this unwanted phase by applying a cancellation π pulse to the unused qubits halfway through the free evolution period between the two BSB pulses, similar to a spin-echo technique. For example, we obtained a process fidelity of $F_p=0.980$ in a three qubit/resonator system where the frequency of the third unused qubit was 7 GHz, its coupling to the resonator was 0.1 GHz, and the microwave frequency of the decoupling pulse was 6.9973 GHz. The other system conditions were similar to that used in the two-qubit simulation found in Sec. IV.

Our process fidelities indicate that our C-NOT gate is stable even with a third qubit in the system, an important property for the system to be scalable. Although simulations have shown that our pulse sequence causes small amounts of "qubit leakage" (Fig. 4), this leakage is minuscule, indicating that we have an extremely well-confined system. This directly results in the gate fidelity being higher than currently achieved by other experimental systems (see for example Riebe *et al.*[37] and their Table II). For large-scale quantum information processing (QIP), however, we have to additionally take more exact measures into account. In the next section, we briefly discuss how we can suppress the qubit leakage even further to meet the criteria for large-scale QIP.

VI. IMPLICATIONS FOR LARGE-SCALE QIP

The simulations presented here for a basic "top-hat" control sequence for the qubit/resonator system have already demonstrated extremely good confinement and, if experimentally achievable, are a major step forward in the fabrication of viable systems for large-scale QIP. Within the context of large-scale QIP, ultrahigh fidelities are required to satisfy the threshold requirements for concatenated error correction and leakage presents a special type of error channel requiring specialized correction.

One of the fundamental assumptions of quantum error correction (QEC) is that errors affecting qubits are localized to the two levels associated with the qubit encoding. Once errors begin to violate this assumption, either through state leakage or actual qubit loss, additional mechanisms must be employed, at the encoding level, to allow for correction.[42–48] Unfortunately, these techniques are quite cumbersome and involve specialized protocols that go beyond the standard operations to realize QEC.

Ideally, for large-scale qubit applications, we do not want to correct for qubit leakage, instead we wish to suppress it to a sufficient level where it can be ignored. This "target" error rate, often referred to as the "fault-tolerant threshold" is highly dependent on the underlying physical architecture and can be anywhere between 10^{-3} and 10^{-7},[49,50] depending on the specific system under consideration. The important point to realize is that if we wish to ignore coherent leakage errors these channels need to be suppressed several orders of magnitude below other standard error channels. Fortunately, the qubit leakage in our gate is due to coherent excitation to

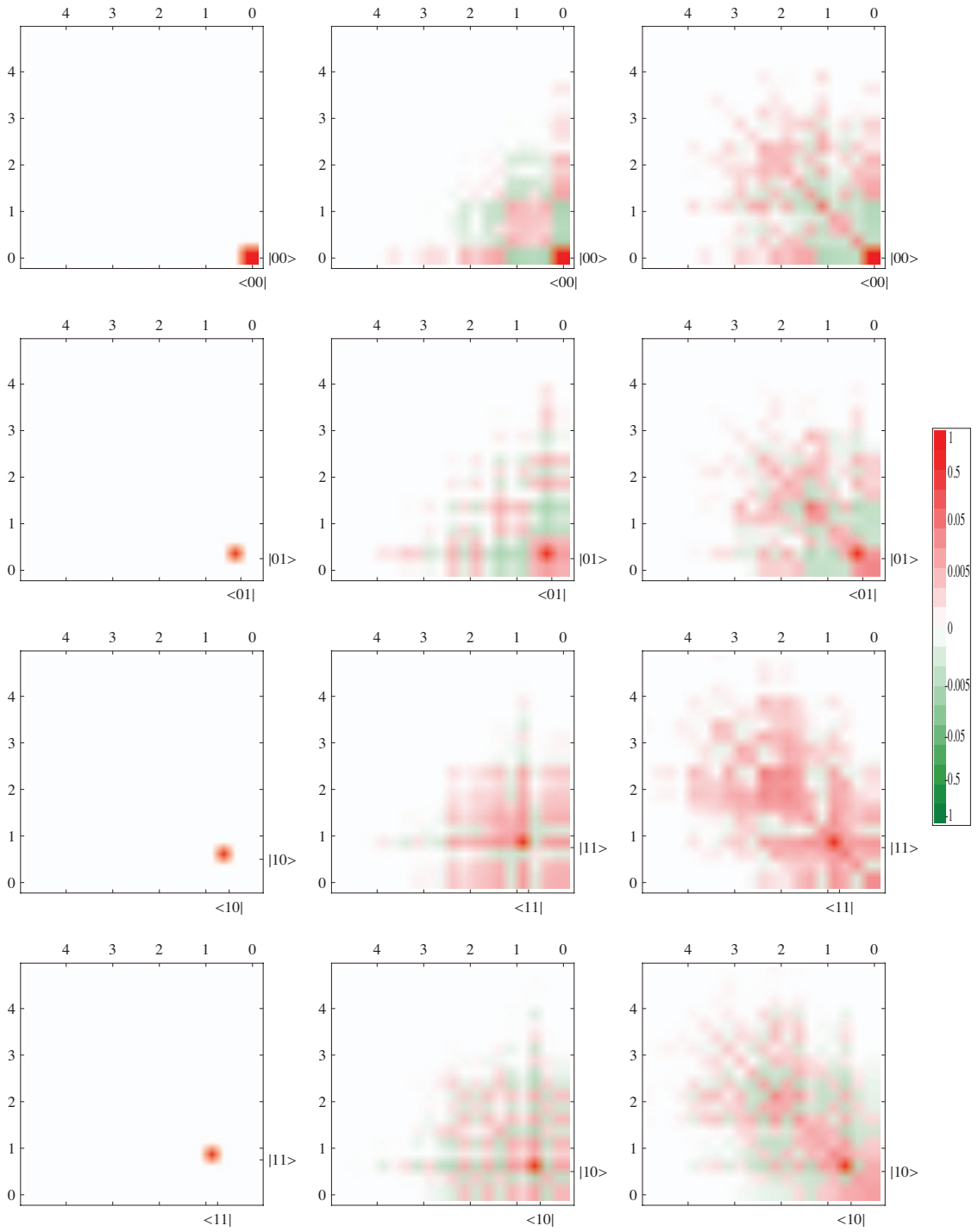

FIG. 4. (Color) From top: initial (left) and final (middle and right) density matrices (real components only) showing the $|00\rangle \mapsto |00\rangle$, $|01\rangle \mapsto |01\rangle$, $|10\rangle \mapsto |11\rangle$, and $|11\rangle \mapsto |10\rangle$ operations, and the corresponding qubit leakage into higher resonator modes ($n > 0$) due to the pulse sequence values defined in Sec. IV without (middle) and with (right) decoherence ($Q = 10^6$ and $\Gamma_1 = \Gamma_2 = 0.25$ MHz). The color scheme used is a nonlinear gradient: zero values are white with negative values greenish and positive values reddish.

higher-order resonator levels. Hence, if we can suppress the unwanted excitation, we could eliminate the qubit leakage.

In more detail, analysis of our pulse sequence indicates that our qubit leakage is initiated by our first BSB pulse on the control qubit. Since the second BSB pulse on the same qubit is only different by a phase, we only require a modified version of the first BSB pulse to avoid leaking population into higher levels of the harmonic oscillator. Moreover, since it is already very well confined, we feel that it represents a good first approximation to a zero leakage modification using optimal quantum-control techniques.

Optimal quantum control,[51–55] first developed in the fields of nuclear magnetic resonance and quantum chemistry, has shown promise as a technique for designing ultrahigh-fidelity control processes for QIP (Refs. 54 and 56–59) and specifically addressing the leakage problem in superconducting

systems.[60] This technique, requiring the application of a second control field, which is approximately the time derivative of the primary, appears to suppress leakage errors by several orders of magnitude. However, further work is needed to extend this work to a qubit-bus-qubit controlled interaction and to ensure that these additional leakage suppression pulses does not induce cross talk or other unwanted dynamics.

Our future work will involve utilizing these numerical techniques to find smooth control field parameters that modify the above simulated BSB pulse to one that eliminates leakage to higher-order field modes. Initial success of these techniques for superconductors,[58,61] ion traps,[58] vibrational modes in molecules,[57] and more general problems in quantum control[53] allows for optimism that this avenue of investigation will eliminate leakage in this system.

VII. CONCLUSIONS

In this paper we have proposed a realizable microwave pulse sequence that effects a C-NOT gate operation on a Josephson-junction-based flux qubit/resonator system with high process fidelity. Our simulations have shown that a C-NOT gate process fidelity of 0.988 (0.980) for a two (three) qubit/resonator system under ideal conditions and a fidelity of 0.903 for a two-qubit/resonator system under the best, currently achieved, experimental conditions, is possible. We have also shown that this set of pulses, in particular, the first BSB pulse, incites minuscule qubit leakage into the first and second excited states of the coupling resonator. The observed leakage in this system represents no serious obstacle to our current experimental efforts. However, within the context of large-scale QIP applications, it would be preferable to suppress the minor population leakage during the first BSB control pulse to the point where leakage correction can be ignored. This will be achieved with optimally constructed multiqubit/resonator gate sequences, architectural specific analysis of the techniques introduced in Ref. 60, as well as modifications to the architecture. Future work will also look into more accurately modeling the dynamical impact of the various low- and high-frequency noise sources inherent in our system,[62] using a more generalized open quantum-system treatment.[63]

ACKNOWLEDGMENTS

We would like to thank W. J. Munro, H. Nakano, T. P. Spiller, and J. E. Mooij for numerous, useful discussions and The Center for Complex Quantum Systems at The University of Texas at Austin for their continued support and encouragement. This work was supported in part by Grant-in-Aid for Scientific Research of Specially Promoted Research under Grant No. 18001002 by MEXT, Grant-in-Aid for Scientific Research (A) under Grant No. 18201018 by JSPS.

*s-saito@will.brl.ntt.co.jp
†ttilma@nii.ac.jp

[1] D. P. DiVincenzo, Science **270**, 255 (1995).
[2] D. P. DiVincenzo, Fortschr. Phys. **48**, 771 (2000).
[3] T. P. Spiller, W. J. Munro, S. D. Barrett, and P. Kok, Contemp. Phys. **46**, 407 (2005).
[4] J. I. Cirac and P. Zoller, Phys. Rev. Lett. **74**, 4091 (1995).
[5] E. Knill, R. Laflamme, and G. J. Milburn, Nature (London) **409**, 46 (2001).
[6] P. Kok, W. J. Munro, K. Nemoto, T. C. Ralph, J. P. Dowling, and G. J. Milburn, Rev. Mod. Phys. **79**, 135 (2007).
[7] D. G. Cory, A. F. Fahmy, and T. F. Havel, Proc. Natl. Acad. Sci. U.S.A. **94**, 1634 (1997).
[8] N. A. Gershenfeld and I. L. Chuang, Science **275**, 350 (1997).
[9] Y. Nakamura, Y. A. Pashkin, and J. S. Tsai, Nature (London) **398**, 786 (1999).
[10] Y. A. Pashkin, T. Yamamoto, O. Astafiev, Y. Nakamura, D. V. Averin, and J. S. Tsai, Nature (London) **421**, 823 (2003).
[11] R. McDermott, R. W. Simmonds, M. Steffen, K. B. Cooper, K. Cicak, K. D. Osborn, S. Oh, D. P. Pappas, and J. M. Martinis, Science **307**, 1299 (2005).
[12] J. H. Plantenberg, P. C. de Groot, C. J. P. M. Harmans, and J. E. Mooij, Nature (London) **447**, 836 (2007).
[13] B. L. T. Plourde, J. Zhang, K. B. Whaley, F. K. Wilhelm, T. L. Robertson, T. Hime, S. Linzen, P. A. Reichardt, C. E. Wu, and J. Clarke, Phys. Rev. B **70**, 140501(R) (2004).
[14] P. Bertet, C. J. P. M. Harmans, and J. E. Mooij, Phys. Rev. B **73**, 064512 (2006).
[15] A. O. Niskanen, Y. Nakamura, and J. S. Tsai, Phys. Rev. B **73**, 094506 (2006).
[16] T. Hime, P. A. Reichardt, B. L. T. Plourde, T. L. Robertson, C. E. Wu, A. V. Ustinov, and J. Clarke, Science **314**, 1427 (2006).
[17] A. O. Niskanen, K. Harrabi, F. Yoshihara, Y. Nakamura, S. Lloyd, and J. S. Tsai, Science **316**, 723 (2007).
[18] A. Blais, J. Gambetta, A. Wallraff, D. I. Schuster, S. M. Girvin, M. H. Devoret, and R. J. Schoelkopf, Phys. Rev. A **75**, 032329 (2007).
[19] H. Nakano, K. Kakuyanagi, M. Ueda, and K. Semba, Appl. Phys. Lett. **91**, 032501 (2007).
[20] T. P. Spiller, K. Nemoto, S. L. Braunstein, W. J. Munro, P. van Loock, and G. J. Milburn, New J. Phys. **8**, 30 (2006).
[21] I. Chiorescu, P. Bertet, K. Semba, Y. Nakamura, C. J. P. M. Harmans, and J. E. Mooij, Nature (London) **431**, 159 (2004).
[22] J. Johansson, S. Saito, T. Meno, H. Nakano, M. Ueda, K. Semba, and H. Takayanagi, Phys. Rev. Lett. **96**, 127006 (2006).
[23] A. Wallraff, D. I. Schuster, A. Blais, L. Frunzio, R. S. Huang, J. Majer, S. Kumar, S. M. Girvin, and R. J. Schoelkopf, Nature (London) **431**, 162 (2004).
[24] M. Hofheinz, E. M. Weig, M. Ansmann, R. C. Bialczak, E. Lucero, M. Neeley, A. D. O'Connell, H. Wang, J. M. Martinis, and A. N. Cleland, Nature (London) **454**, 310 (2008).
[25] M. A. Sillanpää, J. I. Park, and R. W. Simmonds, Nature (London) **449**, 438 (2007).
[26] J. Majer, J. M. Chow, J. M. Gambetta, J. Koch, B. R. Johnson, J. A. Schreier, L. Frunzio, D. I. Schuster, A. A. Houck, A. Wallraff, A. Blais, M. H. Devoret, S. M. Girvin, and R. J. Schoelkopf

Nature (London) **449**, 443 (2007).
[27] L. DiCarlo, J. M. Chow, J. M. Gambetta, L. S. Bishop, B. R. Johnson, D. I. Schuster, J. Majer, A. Blais, L. Frunzio, S. M. Girvin, and R. J. Schoelkopf, Nature (London) **460**, 240 (2009).
[28] F. Brito, D. P. DiVincenzo, R. H. Koch, and M. Steffen, New J. Phys. **10**, 033027 (2008).
[29] J. E. Mooij, T. P. Orlando, L. Levitov, L. Tian, C. H. van der Wal, and S. Lloyd, Science **285**, 1036 (1999).
[30] I. Chiorescu, Y. Nakamura, C. J. P. M. Harmans, and J. E. Mooij, Science **299**, 1869 (2003).
[31] S. Saito, T. Meno, M. Ueda, H. Tanaka, K. Semba, and H. Takayanagi, Phys. Rev. Lett. **96**, 107001 (2006).
[32] P. Bertet, I. Chiorescu, G. Burkard, K. Semba, C. J. P. M. Harmans, D. P. DiVincenzo, and J. E. Mooij, Phys. Rev. Lett. **95**, 257002 (2005).
[33] F. Yoshihara, K. Harrabi, A. O. Niskanen, Y. Nakamura, and J. S. Tsai, Phys. Rev. Lett. **97**, 167001 (2006).
[34] K. Kakuyanagi, T. Meno, S. Saito, H. Nakano, K. Semba, H. Takayanagi, F. Deppe, and A. Shnirman, Phys. Rev. Lett. **98**, 047004 (2007).
[35] P. J. Leek, S. Filipp, P. Maurer, M. Baur, R. Bianchetti, J. M. Fink, M. Göppl, L. Steffen, and A. Wallraff, Phys. Rev. B **79**, 180511(R) (2009).
[36] F. Schmidt-Kaler, H. Häffner, M. Riebe, S. Gulde, G. P. T. Lancaster, T. Deuschle, C. Becher, C. F. Roos, J. Eschner, and R. Blatt, Nature (London) **422**, 408 (2003).
[37] M. Riebe, K. Kim, P. Schindler, T. Monz, P. O. Schmidt, T. K. Körber, W. Hänsel, H. Häffner, C. F. Roos, and R. Blatt, Phys. Rev. Lett. **97**, 220407 (2006).
[38] L. M. K. Vandersypen and I. L. Chuang, Rev. Mod. Phys. **76**, 1037 (2004).
[39] I. L. Chuang and M. A. Nielsen, J. Mod. Opt. **44**, 2455 (1997).
[40] Experimentally, it is not difficult to realize f_{res} of 10 GHz by using a distributed circuit as well as fabricate the flux qubits with gap frequencies f_1 and f_2 around 5 GHz. If we assume that a coplanar strip line resonator, via an insulating layer, overlaps the qubits, we need a mutual inductance M of 10 pH to achieve the couplings g_1 and g_2 of 0.1 GHz, which is satisfied with a qubit loop size of 1.5 μm by 10 μm. Here we assume that the self-inductance of one of the strip lines is 10 nH and the persistent current in the qubit is 350 nA. The loop size is larger than the conventional design but we have already achieved experimentally a qubit relaxation time T_1 of 2 μs and a coherence time T_2 of 2 μs, at the degeneracy point of the flux qubit, with this loop size.
[41] F. G. Paauw, A. Fedorov, C. J. P. M. Harmans, and J. E. Mooij, Phys. Rev. Lett. **102**, 090501 (2009).
[42] J. Preskill, *Introduction to Quantum Computation* (World Scientific, Singapore, 1998), pp. 213–269.
[43] M. Grassl, T. Beth, and T. Pellizzari, Phys. Rev. A **56**, 33 (1997).
[44] J. Vala, K. B. Whaley, and D. S. Weiss, Phys. Rev. A **72**, 052318 (2005).
[45] K. Khodjasteh and D. A. Lidar, Phys. Rev. A **68**, 022322 (2003).
[46] C. Mochon, Phys. Rev. A **69**, 032306 (2004).
[47] L. A. Wu, M. S. Byrd, and D. A. Lidar, Phys. Rev. Lett. **89**, 127901 (2002).
[48] M. S. Byrd, D. A. Lidar, L. A. Wu, and P. Zanardi, Phys. Rev. A **71**, 052301 (2005).
[49] P. Aliferis, F. Brito, D. P. DiVincenzo, J. Preskill, M. Steffen, and B. M. Terhal, New J. Phys. **11**, 013061 (2009).
[50] A. M. Stephens, A. G. Fowler, and L. C. L. Hollenberg, Quantum Inf. Comput. **8**, 330 (2008).
[51] R. S. Judson and H. Rabitz, Phys. Rev. Lett. **68**, 1500 (1992).
[52] V. F. Krotov, *Global Methods in Optimal Control Theory* (Marcel Dekker, New York, 1996).
[53] N. Khaneja, T. Reiss, C. Kehlet, T. Schulte-Herbrüggen, and S. J. Glaser, J. Magn. Reson. **172**, 296 (2005).
[54] T. Schulte-Herbrüggen, A. Spörl, N. Khaneja, and S. J. Glaser, Phys. Rev. A **72**, 042331 (2005).
[55] S. G. Schirmer, I. C. H. Pullen, and A. I. Solomon, J. Opt. B: Quantum Semiclassical Opt. **7**, S293 (2005).
[56] T. Schulte-Herbrüggen, A. Spörl, R. Marx, N. Khaneja, J. M. Myers, A. F. Fahmy, and S. J. Glaser, *Lectures on Quantum Information* (WILEY-VCH Verlag GmbH, Germany, 2007), pp. 481–501.
[57] C. M. Tesch and R. de Vivie-Riedle, Phys. Rev. Lett. **89**, 157901 (2002).
[58] P. Rebentrost and F. K. Wilhelm, Phys. Rev. B **79**, 060507(R) (2009).
[59] V. Nebendahl, H. Häffner, and C. F. Roos, Phys. Rev. A **79**, 012312 (2009).
[60] F. Motzoi, J. M. Gambetta, P. Rebentrost, and F. K. Wilhelm, Phys. Rev. Lett. **103**, 110501 (2009).
[61] A. Spörl, T. Schulte-Herbrüggen, S. J. Glaser, V. Bergholm, M. J. Storcz, J. Ferber, and F. K. Wilhelm, Phys. Rev. A **75**, 012302 (2007).
[62] F. Deppe, M. Mariantoni, E. P. Menzel, S. Saito, K. Kakuyanagi, H. Tanaka, T. Meno, K. Semba, H. Takayanagi, and R. Gross, Phys. Rev. B **76**, 214503 (2007).
[63] C. A. Rodriguez-Rosario and E. C. G. Sudarshan, arXiv:0803.1183 (unpublished).